Scientific Reports

https://doi.org/10.1038/s41598-026-44391-x

Article in Press

Vaccine-derived T-cell responses are insufficient to generate protective immunity to SARS-CoV-2

Received: 19 November 2025

Accepted: 11 March 2026

Published online: 20 March 2026

Cite this article as: Cha S., Szymura S.J., Anderson A. *et al.* Vaccine-derived T-cell responses are insufficient to generate protective immunity to SARS-CoV-2. *Sci Rep* (2026). https://doi.org/10.1038/s41598-026-44391-x

Soung-Chul Cha, Szymon J. Szymura, Aaron Anderson, Zhenyuan Dong, Anmol Kandel, Elizabeth Oh, Michael Palmer, Kevin Arango, Jibin Zhang & Larry W. Kwak

Vaccine-derived T-cell responses are insufficient to generate protective immunity to SARS-CoV-2.

Soung-Chul Cha, Szymon J Szymura, Aaron Anderson, Zhenyuan Dong, Anmol Kandel, Elizabeth Oh, Michael Palmer, Kevin Arango, Jibin Zhang, Larry W Kwak.

Corresponding author: Soung-chul Cha,
Email: socha@coh.org

Stephenson Lymphoma Center, Hematologic Malignancies Research Institute, Beckman Research Institute and City of Hope, Duarte, CA, USA.

Abstract

Neutralizing antibodies are established correlates of protection against SARS-CoV-2, yet T-cell responses are also thought to contribute substantially to limiting disease severity and enhancing durability of protection. To examine whether cellular immunity alone can confer protection, we engineered DNA vaccines encoding modified Spike proteins, including C-terminal truncation (SARS-CoV-2-ΔC, ΔC) and cleavage-site–deleted, linker-inserted (SARS-CoV-2-Linker-ΔT, Linker-ΔT) variants, with or without genetic fusion to MIP3α, which has been shown to enhance targeting of antigen-presenting cells (APC) and preferentially induce T-cell responses. In BALB/c mice, ΔC constructs induced non-neutralizing Spike- and RBD-binding antibodies across variants, as well as robust CD4+ and CD8+ T cell responses, whereas Linker-ΔT elicited strong Th1-skewed cellular immunity in the absence of humoral responses. In K18-hACE2 mice antibody neutralizing activity was not detected by any of the vaccines, and none conferred protection following lethal virus challenge, despite robust specific T-cell cytokine responses. These findings support chemokine-fusion strategies to enhance T cell priming, while indicating that the cellular immunity elicited by this vaccine alone does not confer protection against SARS-CoV-2. Integrating such APC-targeting strategies with structural modifications that preserve pre-fusion neutralizing epitopes may be worthwhile.

Introduction

Early innate immune responses, including interferon signaling and myeloid activation, critically influence SARS-CoV-2 disease severity[1] and shape the magnitude and durability of subsequent adaptive and vaccine-induced immunity[2]. The development of safe and effective vaccines against SARS-CoV-2 has relied largely on immunogens capable of eliciting high titers

of neutralizing antibodies, as exemplified by mRNA and adenoviral platforms. Neutralizing antibody levels strongly correlate with protection in both non-human primates and humans, serving as the principal mechanistic correlate of immunity[3,4]. However, accumulating evidence suggests that T-cell responses also play an important role, particularly in limiting disease severity and sustaining long-term protection as antibody titers wane[5-7]. The extent to which T-cell immunity can compensate for deficient neutralizing antibody responses remains a central unresolved question. This issue has particular clinical relevance for patients with B-cell malignancies or those receiving B-cell–depleting therapies, in whom antibody formation after SARS-CoV-2 vaccination is frequently impaired while T-cell responses are often preserved. Understanding the balance between these immune mechanisms is therefore critical for guiding vaccine design and optimizing protective strategies in immunocompromised populations.

DNA vaccines provide a flexible platform for rapid antigen engineering and have shown the capacity to induce both humoral and cellular responses in preclinical and clinical settings[5,8]. Nevertheless, the immunogenicity of DNA vaccines is often lower than that of mRNA vaccines, and strategies to improve antigen delivery and immune activation are needed. One such approach involves chemokine fusion, which targets antigens to antigen-presenting cells (APCs), thereby enhancing priming of adaptive immunity[9]. Our group has previously demonstrated that chemokine–antigen fusion DNA vaccines can elicit potent immune responses against infectious pathogens and tumors in preclinical models [9-12], and clinical safety has been established in a first-in-human trial of a lymphoma DNA vaccine [13]. Consistent with prior work in infectious disease and cancer models, MIP3α fusion DNA vaccination drives a Th1-skewed immune profile, with dominant IFNγ and TNFα secretion and minimal induction of Th2-associated cytokines[14]. Therefore, we selected MIP3α as a driver for immature dendritic cells to enhance cellular immunity. We hypothesized that MIP3α fusion to the Spike glycoprotein enhances APC targeting and T-cell priming, supporting cellular immunity as the primary protective mechanism against SARS-CoV-2. Here, we applied this APC-targeted DNA vaccine strategy to SARS-CoV-2. We engineered multiple DNA vaccine constructs encoding the spike glycoprotein (including variants with C-terminal truncation (ΔC), protease cleavage site deletion and linker insertion (Linker-ΔT), with and without fusion to the chemokine MIP3α. By evaluating humoral and cellular immunity in BALB/c and K18-hACE2 mouse models, we show that an APC-targeted MIP3α fusion DNA vaccine elicits robust Th1-biased T cell responses but requires neutralizing antibodies for protection against SARS-CoV-2.

Methods

Vaccine constructs

DNA vaccine plasmids were generated using a preclinical-grade pVax-based backbone. The SARS-CoV-2 Spike (isolate Wuhan-Hu-1; GenBank accession MN908947.3[15]) sequence was codon-optimized for mammalian expression. Three Spike variants were engineered: (i) ΔC, with a 19–amino acid cytoplasmic tail deletion; (ii) Linker-ΔT, with deletion of the S1/S2 and S2′ protease cleavage sites and insertion of a $(G4S)_2$ linker with truncation of the transmembrane and cytoplasmic domains. For APC targeting, murine MIP3α was fused to the N-terminus of each construct via a flexible linker. An HA-tag was included at the C-terminus for detection. An irrelevant control construct encoding MIP3α fused to A20-scFv was also generated. Plasmids were purified under endotoxin-free conditions (Qiagen EndoFree kit) and validated by sequencing and restriction digest.

Animals and immunization

The Institutional Animal Care and Use Committee (IACUC) of the Beckman Research Institute at City of Hope (COH) approved protocol 20032, which is assigned to this study. All study procedures were conducted in strict compliance with the guidelines outlined in the Guide for the Care and Use of Laboratory Animals and the Public Health Service Policy on the Humane Care and Use of Laboratory Animals as well as in accordance to the ARRIVE (Animal Research: Reporting of In Vivo Experiments) guidelines. Mice were maintained on a 12-hour light/12-hour dark cycle at 22–24 °C and 30–70% humidity, with ad libitum access to food and water. Six-week-old BALB/c (BALB/cJ, 000651) or B6.Cg-Tg (K18-ACE2)2Prlmn/J (K18-hACE2, 034860) transgenic mice were obtained from The Jackson Laboratory. Mice were anesthetized with 2–3% isoflurane inhalation for vaccination and blood collection. For terminal tissue harvest, animals were euthanized using CO_2 inhalation followed by cervical dislocation, consistent with AVMA (American Veterinary Medical Association) -approved euthanasia recommendations. Vaccinations were administered via intramuscular injection into the quadriceps using the Tropis injector (PharmaJet), delivering 50 µg or 100 µg of DNA in 50 µL of sterile PBS per dose. A three-dose schedule was implemented on days 0, 14, and 28. Blood samples for humoral immune analysis were collected prior to each immunization, and the mice were euthanized for blood and spleen collection two weeks following the final vaccination. Splenocytes for cellular immune analysis were collected two weeks after booster immunization and isolated using standard procedures following humane euthanasia of the animals.

Serological assays

Sera were collected retro-orbitally prior to each immunization and two weeks post-final immunization. Antibody binding to recombinant SARS-CoV-2 Spike and variant RBD proteins [Ancestral (Wuhan-Hu-1),

Beta (B.1.351), Gamma (P.1), Kappa (B.1.617.1), Delta (B.1.617.2), Alpha (B.1.1.7) ; BEI Resources] was measured by ELISA. Plates were coated with antigen (2 μg/mL), blocked with BSA, and incubated with serially diluted sera. Bound IgG was detected with HRP-conjugated anti-mouse IgG and developed with TMB substrate. Endpoint titers and area under the curve (AUC) were calculated.

SARS-CoV-2 pseudovirus production and neutralization assay

COVID 19 Spike Coronavirus Pseudovirus (MyBioSource, Cat:MBS434275) input was standardized by 100X signal above cell-only background. Heat-inactivated mouse sera were pooled, serially diluted (1:20–1:640), and incubated 1 hour at 37 °C with SARS-CoV-2 spike pseudoviruses. HEK293T-ACE2 cells (2 × 10^4/well) were infected in the presence of 5 μg/mL polybrene, and luciferase activity was quantified 48 h later using Promega reagents. We plotted the data using luminescence vs. virus dilution. Neutralization was calculated as NT = [1 − (RLU immune sera / RLU control)] × 100, with NT90 values interpolated from dilution curves. Neutralizing activity was assessed using serial serum dilutions starting at 1:16, as previously described for SARS-CoV-2 pseudovirus. The assay limit of detection was defined as the lowest serum dilution tested (1:16), below which neutralizing activity could not be reliably quantified. The method was adapted from Crawford, H.D. et al[16] and Chiuppesi F et al [17].

T-cell analysis

Splenocytes were collected two weeks after the final immunization and prepared by mechanical dissociation followed by red blood cell lysis. Cells were rested overnight in complete RPMI 1640 supplemented with 10% fetal bovine serum, 1% penicillin–streptomycin, 2 mM L-glutamine, and 50 μM 2-mercaptoethanol. For functional assays, 1–2 × 10^6 splenocytes per well were stimulated with overlapping peptide pools covering the SARS-CoV-2 Spike protein (Miltenyi Biotec; S or S1 peptide pools; 1–2 μg/mL per peptide) or with an irrelevant CMV peptide pool as a negative control. Stimulations were performed in the presence of brefeldin A and monensin for 5–6 h at 37 °C with 5% CO_2. Following stimulation, cells were stained with fixable viability dye and antibodies against CD3, CD4, and CD8. After fixation and permeabilization (BD Cytofix/Cytoperm), intracellular cytokine staining was performed with antibodies specific for IFN-γ, TNF-α, IL-2, IL-4, and IL-5. Data were acquired on a BD LSRFortessa flow cytometer, and ≥100,000 lymphocyte events were collected per sample. FlowJo 10.8.1 (BD Life Sciences) was used for analysis. Gating was applied sequentially on singlets, live $CD3^+$ T cells, and $CD4^+$ or $CD8^+$ subsets, with cytokine-positive populations quantified. Boolean gating was used to define polyfunctional subsets expressing one or more cytokines simultaneously.

Concurrently, splenocytes were evaluated using cytokine ELISA, with splenocytes from immunized mice plated at a density of 5 x 10^6 cells per well in 24-well plates. The cells were stimulated with overlapping peptide pools spanning the SARS-CoV-2 Spike protein (Miltenyi Biotec; S or S1 peptide pools; 1–2 µg/mL per peptide) or with an irrelevant CMV peptide pool as a negative control, and incubated at 37 °C for 3 days. The supernatant was collected and analyzed to assess cytokine production. Mouse IFNγ, IL-6, IL-2, TNFα, IL-4, and IL-5 were quantified by ELISA using the corresponding antibody sets (Invitrogen) in accordance with the manufacturer's instructions.

SARS-CoV-2 wildtype virus neutralization assay and challenge in K18-hACE2 mice

All procedures were carried out in strict compliance with the NIH Guide for the Care and Use of Laboratory Animals and were approved by the Institutional Animal Care and Use Committee (IACUC) at Bioqual, Inc. Bioqual acquired 64 K18-hACE2 mice (32 males and 32 females) from Jackson Laboratory, which were subsequently randomly assigned to four experimental groups (n=16 per group). The animals were immunized on Study Days (SD) 0, 14, and 28, in accordance with the prescribed vaccination schedule, dosage, formulation, and route of administration described above in the method. No deviations or modifications to the vaccination protocol were applied for animals contributing sera to the neutralization studies. On SD41, six mice per group (three males and three females) were humanely euthanized for terminal blood collection and splenectomy, while the remaining animals underwent interim blood sampling. Serum samples were subsequently analyzed by Bioqual through a plaque reduction neutralization test (PRNT). Body weight was recorded at baseline, prior to each immunization, and daily during viral challenge studies.

Serum samples from each experimental group were sent to City of Hope for independent ELISA-based assessment of antibody binding to the SARS-CoV-2 Spike protein, to verify Spike-specific antibody recognition in the vaccinated groups. Surviving mice in SD48 were intranasally inoculated with 2.8 × 10^3 PFU of live SARS-CoV-2 WAS-Calu-3 (lot #12152020-1235). During the study period, mice were monitored for weight loss and clinical manifestations of disease. On SD64, all remaining animals were humanely euthanized, and their spleens were collected for subsequent flow cytometry and ELISpot analyses.

IFN-γ ELISpot assay

Antigen-specific T cell responses were evaluated using an IFN-γ ELISpot assay conducted by Bioqual in accordance with established standard operating procedures. Briefly, splenocytes were plated in duplicate or triplicate at 2–3 × 105 cells per well on PVDF-backed 96-well plates pre-coated with anti–mouse IFN-γ capture antibody. Cells were stimulated with overlapping peptide pools encompassing the SARS-CoV-2 Spike protein (Miltenyi Biotec; S or S1 peptide

pools at 1–2 µg/mL per peptide), while unstimulated wells served as negative controls and wells treated with Concanavalin A (ConA) were included as positive controls. After incubation for approximately 18–24 hours at 37 °C in a 5% CO_2 atmosphere, the plates were washed and subsequently incubated with a biotinylated anti–IFN-γ detection antibody, followed by treatment with a streptavidin–enzyme conjugate and substrate development. Spot-forming units (SFU) were quantified using an automated ELISpot reader, and the results were expressed as SFU per 10^6 cells after subtracting background spots from unstimulated control wells.

Statistical analysis

All statistical analyses were conducted using GraphPad Prism version 9. For comparisons between two groups, the two-tailed Mann–Whitney U test was used, as data did not consistently meet assumptions of normality and sample sizes were limited. as appropriate. Survival curves were compared using the log-rank (Mantel–Cox) test. $P < 0.05$ was considered statistically significant. All data are presented as mean ± SEM.

Results

SARS-CoV-2 DNA Vaccine design

The Spike glycoprotein (S-protein) of the SARS-CoV-2 (isolate Wuhan-Hu-1; GenBank accession MN908947.3[18]) virion was codon optimized and inserted into a pVax-based DNA vaccine vector (Fig. 1A). A leader sequence derived from the interferon-induced protein 10 (IP-10) was engineered and inserted at the N-terminus of the spike glycoprotein to facilitate its secretion through the rough endoplasmic reticulum membrane during protein synthesis [9]. Additionally, a hemagglutinin tag (HA-tag) was incorporated into each design to serve as a universal epitope tag.

We designed DNA vaccines to encode four codon optimized SARS-CoV-2 DNA spike proteins, with and without murine MIP3α fusion. First, we constructed a full-length spike protein construct with 19 amino acids (KFDEDDSEPVLKGVKLHYT) removed from the CT (pSARS-CoV-2-ΔC) and a fusion of (pMIP3α-SARS-CoV-2-ΔC). We also deleted the TM and CT, further hypothesized that deleting the protease sites and inserting $(G_4S)_2$ linkers would disrupt epitope folding and thereby abrogate antibody induction, with MIP3α (*pMIP3α-SARS-CoV-2-Linker-ΔT*) or without MIP3α (*pSARS-CoV-2-Linker-ΔT*). A DNA vaccine encoding A20 lymphoma scFv with irrelevant specificity (pMIP3α-A20-scFv) was used as a negative control[12].

pSARS-CoV-2-ΔC DNA vaccine immunogenicity in BALB/c mice

We first characterized immunogenicity of the various DNA vaccines in BALB/c mice. Doses of either 50 µg or 100 µg of pSARS-CoV-2-ΔC and pMIP3α-SARS-CoV-2-ΔC vaccines were administered by Tropis injector to deliver uniform vaccine administration. Mice were serially immunized three times, with a 2-week interval between each vaccination. Blood samples were collected before each immunization, and the mice were euthanized for blood and spleen collection 2 weeks after the final vaccination (Fig. 2A).

Endpoint humoral responses were measured by ELISA and demonstrated antibody binding to the SARS-CoV-2 Spike protein by all mice in both groups (Fig 2B). Area under the curve calculations revealed no significant differences between pSARS-CoV-2-ΔC and pMIP3α-SARS-CoV-2-ΔC vaccines at either dose level (Supplementary Fig. 1A). Because SARS-CoV-2 recognizes host cell receptors through its receptor-binding domain (RBD), immune sera were also analyzed for their ability to recognize various RBD variants (Supplementary Figure 1B). The results demonstrated that serum antibodies derived from pSARS-CoV-2-ΔC and pMIP3α-SARS-CoV-2-ΔC effectively distinguish between variant RBDs without any substantial differences. While antibodies generated by both vaccines exhibited reactivity against Spike proteins from multiple variants (Fig S1A), they failed to induce neutralizing antibody responses against SARS-CoV-2 pseudovirus (Supplementary Fig. 1C).

T cell responses to SARS-CoV-2 were assessed by stimulating splenocytes isolated from vaccinated mice with Miltenyi Biotec S or S1 peptide pools, while a CMV peptide pool served as the negative control. Cytokine concentrations in culture supernatants were initially quantified using ELISA, revealing robust antigen-specific responses characterized by the production of IFNγ, IL-6, IL-2, TNFα, IL-4, and IL-5 (Fig. 2C). Since supernatant cytokine measurements represent the combined contributions of multiple immune cell types, intracellular cytokine staining was subsequently conducted to identify T cell–specific responses. Both CD4+ and CD8+ T cells stimulated with SARS-CoV-2 Spike peptide pools demonstrated statistically significant increases in the frequency and magnitude of IFNγ and TNFα expression compared to control stimulation, while IL-2 expression was undetectable. No significant differences were observed between the responses of CD4+ T cells (Fig. 2D) and CD8+ T cells (Fig. 2E). Representative flow cytometry plots illustrating the gating strategy and intracellular cytokine staining are provided in Supplementary Fig. 4.

pSARS-CoV-2-Linker-ΔT DNA vaccine immunogenicity in BALB/c mice

Our central hypothesis was that cellular immunity, rather than humoral immunity, constitutes the dominant protective mechanism against SARS-CoV-2. Linker-ΔT constructs were designed to disrupt optimal prefusion spike conformation, thereby potentially diminishing antibody titers while preserving, or even enhancing, T cell–mediated immunity. Humoral and cellular

immunity of pSARS-CoV-2-Linker-ΔT vaccines, with and without MIP3 fusion, were also evaluated at 50 µg and 100 µg doses. As expected, antibody binding to the SARS-CoV-2 spike protein was not detected in the serum samples collected from mice vaccinated with either construct or at either dose (Fig 3B). In contrast, Linker-ΔT vaccines induced specific T-cell responses. Splenocytes from mice vaccinated with either construct produced significant levels of IFNγ, IL-6, IL-2, and TNFα in culture supernatants by ELISA, with no substantial differences between the two constructs of doses (Fig. 3C). Intracellular cytokine analysis of peptide-restimulated splenocytes revealed a predominantly Th1-skewed response, especially in mice vaccinated with the MIP3 fusion (Fig. 3DE). For example, pMIP3α-SARS-CoV-2-Linker-ΔT vaccine induced significant TNFα and IFNγ production in $CD4^+$ and $CD8^+$ T cells at either dose, while less IL-2 production was observed. Moreover, in $CD4^+$ T cells, significant IFNγ production was observed exclusively in the pMIP3α groups at both doses (Fig. 3D).

.

Vaccine immunogenicity in K18-hACE2 mice

With the eventual goal of testing for virus protection, we extended immunogenicity experiments to K18-hACE2 transgenic mice that express human angiotensin-converting enzyme 2 (ACE2), the receptor exploited by SARS-CoV-2 for cellular entry. Female k18-hACE2 mice (N = 5) were first immunized with 100 µg of the pMIP3α-SARS-CoV-2-ΔC or pSARS-CoV-2-ΔC DNA vaccines diluted in 50µL of sterile phosphate buffered saline (PBS) on days 0, 14, and 28, as before (Fig 4A). Compared with pSARS-CoV-2-ΔC, mice vaccinated with pMIP3α-SARS-CoV-2-ΔC exhibited a trend towards higher serum antibody responses against the S protein (Fig. 4B). Moreover, serum antibody responses against Ancestral (Wuhan-Hu-1), Beta (B.1.351), Gamma (P.1), Kappa (B.1.617.1), Delta (B.1.617.2), and Alpha (B.1.1.7) RBD variants were more robust in the pMIP3α-SARS-CoV-2-ΔC group (Supplementary Fig. 2A). However, neutralizing antibodies were not consistently detected in mice vaccinated with either pMIP3α-SARS-CoV-2-ΔC or pSARS-CoV-2-ΔC (Fig. 4C).

Robust specific Splenocytes responses were detected in both groups, as analyzed by cytokine production by ELISA. Specifically, splenocytes from mice vaccinated with either pSARS-CoV-2-ΔC or pMIP3α-SARS-CoV-2-ΔC and stimulated with the SARS-CoV-2 Spike peptide pool produced statistically significant levels of IFNγ, IL-6, IL-2, TNFα, IL-4, and IL-5, compared with those stimulated with negative controls (CMV peptide pools; Fig 4D). Specific IFNγ production by stimulated splenocytes from both pSARS-CoV-2-ΔC and pMIP3α-SARS-CoV-2-ΔC groups was also detected by intracellular staining, particularly from CD8+ cells (Fig 4E).

Antigen-targeting DNA vaccine–derived T cell responses without neutralizing antibodies were nonprotective in K18-hACE2 mice.

We designed a second experiment to investigate both immunogenicity and virus protection in K18-hACE2 mice, including both vaccines above and adding the pMIP3α-SARS-CoV-2-Linker-ΔT vaccine (Fig 5A). Sixteen mice per group were vaccinated with 100 micrograms pSARS-CoV-2-ΔC, pMIP3α-SARS-CoV-2-ΔC, pMIP3α-SARS-CoV-2-Linker-ΔT, or pMIP3α-A20-scFv (negative control) in three doses administered as above. Two weeks after the final vaccination, six mice from each experimental group were euthanized for terminal bleeding and splenocyte isolation. The remaining ten mice were retro-orbitally bled, subsequently challenged with 2.8×10^3 PFU of WAS-Calu-3 (LOT #12152020-1235) ten days later, and then monitored for variations in body weight and survival. As anticipated, mice vaccinated with both SARS-CoV-2-ΔC vaccines, but especially those vaccinated with the MIP3 fusion, demonstrated significant increases in serum antibody titers against the S protein (Fig 5B, S3 Fig). However, corresponding neutralizing antibody activity against live SARS-CoV-2 virus was not observed in any of the groups (Fig 5C). T-cell responses analyzed by intracellular cytokine staining for TNFα, IL-2, and IFNγ showed significant responses after stimulation with SARS-CoV-2 Spike protein peptide pools (S), compared with negative control stimulation (CMV) by both CD4+ and CD8+ T cells (Fig 5D). Specific IFNγ production was also detected by all three vaccines by ELISPOT (Fig 5E).

Compared with negative controls, none of the experimental vaccines protected against weight loss or death (Fig. 5F and G). Our results indicate that T cell responses elicited by the MIP3α fusion DNA vaccine alone were insufficient to confer protection against SARS-CoV-2 in K18-hACE2 mice.

Discussion

Building upon our previous studies demonstrating that the genetic fusion of chemokines to tumor antigens enhances antigen cross-presentation and induces robust $CD8^+$ and Th1-type T-cell immunity in cancer models, we have applied this principle to the design of a vaccine for infectious diseases by leveraging MIP3α-mediated targeting of immature dendritic cells to augment cellular immunity against SARS-CoV-2.

To test the hypothesis that T-cell responses against SARS-CoV-2 are necessary and sufficient for protection against this virus, we investigated the immunogenicity of several different SARS-CoV-2 DNA vaccine prototypes, designed to primarily induce T-cell immunity.

All vaccine candidates induced robust CD4+ and CD8+ T cell responses characterized by specific cytokine production. Moreover, Spike- and RBD-binding antibodies were consistently detected across constructs and recognized multiple viral variants; however, none of the vaccines elicited neutralizing antibodies or conferred protection against lethal viral challenge. These findings suggest that neutralizing antibodies may be required for virus protection.

Our findings align with large-scale correlates of protection analyses, which demonstrate that neutralizing antibody titers serve as the most reliable quantitative predictors of vaccine efficacy against SARS-CoV-2 infection. For example, Cromer, Vidal, and colleagues demonstrated that neutralizing antibody titers exhibited a strong correlation with protection from symptomatic infection[19,20]. This finding suggests that T-cell immunity alone is insufficient to prevent viral entry. Consistent with depletion studies in macaques [4] and K18-hACE2 mice[21] showing that $CD8^+$ T cells contribute to viral control but provide limited protection from disease, our findings align with clinical studies in immunocompromised patients indicating that passive administration of neutralizing monoclonal antibodies or convalescent plasma is associated with improved clinical outcomes and enhanced viral clearance despite preserved T cell responses [22] [23]. Collectively, these findings indicate that while T-cell immunity serves an important supportive function, neutralizing antibodies are a critical determinant of protection against SARS-CoV-2, particularly in rigorous disease models

Our study's findings corroborate this conclusion, as robust T-cell cytokine responses were not protective in the absence of neutralizing antibodies. Our observations also corroborate findings in rhesus macaques, where passive transfer of IgG alone was sufficient to confer protection against challenge, while CD8+ T cells contributed only when neutralizing antibody titers were subprotective[20].

Nonetheless, the breadth and functionality of T-cell responses are likely to play crucial roles in mitigating disease severity following infection. Vaccine-induced T cells have been shown to maintain 70–80% of their epitope recognition across the Omicron variant and other variants, despite substantial reductions in neutralization capacity [24] thereby providing a critical immunological “backstop” against viral evolution. Clinical data further reinforce this paradigm: early and polyfunctional T-cell responses are correlated with milder clinical outcomes, and in B-cell–depleted patients, preserved T-cell responses following vaccination are associated with a reduced risk of severe disease [25]. The absence of neutralizing antibodies remains a critical vulnerability, addressed clinically through timed revaccination, monoclonal antibody prophylaxis, early antivirals, and occasionally convalescent plasma[26,27].

Furthermore, other DNA vaccine platforms have achieved protective efficacy in preclinical models when neutralizing antibodies were elicited. For example, Yu et al. showed that DNA vaccines encoding full-length spike induced both neutralizing antibodies and protection against SARS-CoV-2 in rhesus macaques[28]. Similarly, DNA vaccine delivered with electroporation, elicited both T-cell and neutralizing antibody responses in humans[29,30]. Interestingly, a recent study using an RBD–MIP3α construct demonstrated durable humoral responses lasting at least 12 months in mice, contrasting with the absent neutralization in our ΔC- and Linker-based constructs[31] These discrepancies likely arise from fundamental

differences in antigen design, epitope presentation, and stabilizing mutations. Structure-guided stabilization of the full-length Spike ectodomain—exemplified by the S-2P and HexaPro variants—has been critical in locking the protein in its prefusion conformation, thereby exposing neutralization-sensitive epitopes and enhancing immunogenicity; these advancements have been fundamental to the success of mRNA-1273 and other commercial platforms, consistently eliciting high-titer neutralizing antibodies in both preclinical and clinical studies[32,33]. In contrast, our ΔC and Linker-ΔT constructs incorporated deletions and cleavage-site modifications without stabilizing mutations, alterations that may have compromised the conformational integrity of the RBD and, as a result, limited B cell recognition of neutralizing epitopes. Beyond stabilization, the multivalent display of antigens has emerged as a critical factor influencing vaccine efficacy. Self-assembling nanoparticles displaying multiple copies of the receptor-binding domain (RBD), such as the I53-50 two-component scaffolds, have been demonstrated to induce significantly higher neutralizing titers and broader recognition of variants compared to monomeric RBD or unstabilized Spike construct. Similarly, recombinant prefusion-stabilized Spike proteins, formulated with potent adjuvants such as the saponin-based Matrix-M employed in NVX-CoV2373, have exhibited robust neutralizing activity and demonstrated clinical efficacy[34,35]. Our DNA vaccine constructs lacked these design features—multimerization, prefusion stabilization, and optimized adjuvantation—and instead depended exclusively on plasmid-mediated expression of modified Spike antigens delivered via intramuscular injection.

The protective efficacy of T cells in the absence of neutralization has been reported in other settings. For example, epitope-focused or ubiquitin-targeted DNA vaccines reduced morbidity and mortality in K18-hACE2 mice without detectable neutralizing antibodies[36]. Although DNA vaccines offer advantages in safety and manufacturing flexibility, their immunogenicity is generally lower than that of mRNA vaccine platforms, particularly in human studies [37]. In contrast, mRNA vaccines elicit robust neutralizing antibody and Th1-biased cellular immune responses in humans, underpinning their rapid clinical success against SARS-CoV-2, a feature associated with long-lasting immunity.[38] In contrast, although our MIP3α-targeted DNA vaccines elicited robust cytokine responses, they failed to confer protection, suggesting that the induced T cells may have lacked key qualitative features of protective immunity—such as sufficient clonal diversity, TCR avidity, cytotoxic function, appropriate tissue localization, and memory differentiation—which were not directly assessed in this study.

Future vaccine iterations should therefore aim to enhance T-cell quality through optimized antigen processing and presentation to achieve protective efficacy even in the absence of neutralizing antibodies.

In addition to MIP3α, other chemokines have been investigated as antigen-delivery vehicles to APCs, with distinct immunological consequences. MCP-1 has been shown to stimulate IL-4 production, thereby driving Th2 polarization in a regulatory manner[39,40]. Similarly, the macrophage-derived chemokine CCL22 (MDC) selectively recruits Th2 cells to APCs [40]. MIP3α fusion preferentially induces Th1-driven cellular immunity, optimizing $CD8^+$ effector T-cell responses and IFNγ output, whereas MCP-1 or MDC incorporation tends to bias immunity toward a Th2 phenotype with superior antibody production. Thus, rational chemokine selection provides a potential strategy to tailor immune polarization: Th1-inducing chemokines such as MIP3α may enhance antiviral T-cell responses, whereas Th2-inducing chemokines like MCP-1 or MDC may complement this by boosting antibody responses. In the context of SARS-CoV-2 vaccines, combining or sequentially deploying these chemokine-fusion strategies could theoretically broaden protective immunity by balancing cellular and humoral arms of the adaptive response.

T cell responses elicited by the MIP3α fusion DNA vaccine, designed to target antigen-presenting cells, were insufficient to confer protection against SARS-CoV-2 in a stringent K18-hACE2 mouse challenge model. In contrast to vaccine strategies that Studies conducted by Shi et al[36]**.** have reported that vaccine strategies aimed at optimizing antigen processing and eliciting cytotoxic T lymphocyte responses exhibit protective efficacy against SARS-CoV-2, even when solely dependent on T-cell responses. Accordingly, the lack of protection observed here likely reflects qualitative and contextual differences in the induced T cell responses rather than a fundamental limitation of T cell–mediated immunity. Furthermore, it is important to note that assessments of vaccine efficacy predominantly concentrated on survival rates and weight loss, without evaluating initial viral replication, tissue dissemination, or pulmonary lesions. On the other hand, the K18-hACE2 model represents a highly stringent and neuroinvasive system, characterized by rapid viral dissemination and central nervous system involvement. Under these conditions, immune mechanisms that may contribute to partial protection, disease modulation, or delayed pathology—such as T-cell–mediated immunity in the absence of neutralizing antibodies—risk being overlooked or underestimated.

Our study demonstrates that although MIP3α fusion DNA vaccines elicit robust Th1-biased T cell responses and broaden Spike-binding antibody responses, induction of neutralizing antibodies remains indispensable for protection against SARS-CoV-2. These findings have direct implications for immunocompromised populations, such as individuals with B cell depletion, in whom antibody responses are impaired despite preserved T cell immunity. Accordingly, future vaccine strategies may benefit from combining Th1- and Th2-inducing chemokine fusions with antigen designs that promote efficient antigen processing and cytotoxic T lymphocyte activation, thereby optimizing both neutralizing antibody quality and durable cellular immunity.

Figure Legends

Figure 1. Design of DNA Vaccines. (A) Schematic diagram of the full-length Spike glycoprotein of the SARS-CoV-2 virion. The spike glycoprotein, composed of the S1 and S2 subunits, comprises the N-terminal domain (NTD), the receptor-binding domain (RBD), subdomain 1(SD1), subdomain (SD2), heptad repeat 1(HR1), central helix (CD), heptad repeat 2 (HR2), transmembrane domain (TM), and cytoplasmic tail (CT). **(B)** Four different DNA vaccines encoding variations of the SARS-CoV-2 Spike (S) protein were constructed: (i) full–length Spike (*pSARS-CoV-2-ΔC; ΔC*: KFDEDDSEPVLKGVKLHYT removed from the CT), (ii) addition of the chemoattractant MIP3α to the *ΔC* Spike (*pMIP3α-SARS-CoV-2-ΔC*), (iii) the deletion of the TM and CT from Spike with the addition of two disulfide linkers $(G4S)_2$ at the ΔS1/S2 and ΔS2' cleavage sites of the Spike with MIP3α (*pMIP3α-SARS-CoV-2-Linker-ΔT*) and without MIP3α (*p SARS-CoV-2-Linker-ΔT*). The pMIP3α-A20-scFv vaccine encodes the A20 mouse tumor idiotype as a negative control with irrelevant specificity. All DNA vaccine inserts were cloned into the pUCMVC3 DNA Vaccine backbone which included a CMV promoter.

Figure 2. SARS-CoV-2 DNA vaccines drive cellular immunity and binding antibodies but no detectable neutralization

(A) BALBC/J wild type mice (N = 45) mice were intramuscularly immunized with 3 doses of either 50 or 100 µg at 2-week intervals using a mouse modified Pharmajet Tropis Needle free Injector with either the pMIP3α-SARS-CoV-2-ΔC or pSARS-CoV-2-ΔC. Mice were immunized with PBS as a negative control. The timeline shows the bleeding and immunization regiment. Humoral immune responses were assessed using binding antibody ELISA to the Spike protein on serum isolated from blood collected at experimental endpoint**. (B).** Humoral responses in each group injected with different vaccine or dose measured by ELISA. Mice showing elicited Spike binding were color coded and matched to their corresponding number in the experimental group. **(C)** Cytokine concentrations in culture supernatants from antigen-stimulated **splenocytes** were measured by ELISA. Cellular Immune response was measured using cytokine staining assays for splenocytes collected at experimental endpoint in response to pooled S peptides for IFNγ, IL-6, IL-2, TNFα, IL-4, and IL-5. Phorbol 12-myristate 13-acetate (PMA) was used as positive control, non-treated (NT) cells served as a negative control, and CMV peptides were included as an irrelevant control. **(D, E)** TNFα, IL-2, and IFNγ Intracellular staining for CD4+ and CD8+ T cells collected at experimental endpoint for assessing cellular immune responses induced by the DNA vaccines. Data representative of two independent

experiments. Values are presented as mean ± standard deviation. *P* values were determined using the Mann-Whitney test. * $0.01 < p < 0.05$, ** $0.01 < p < 0.001$, *** $0.001 < p < 0.0001$. **** $p < 0.0001$.

Figure 3. SARS-CoV-2 DNA Linker-ΔT Vaccine induces T cell Responses but not Humoral Responses to SARS-CoV-2 S Protein. (A) BALBC/J wild type mice (N = 50) mice were intramuscularly immunized with 3 doses of either 50 or 100 µg of either the pMIP3α-SARS-CoV-2-Linker-ΔT or the pSARS-CoV-2-Linker- ΔT DNA Vaccine at 2-week intervals using a mouse modified Pharmajet Tropis Needle free Injector. The Linker-ΔT construct encodes for a disulfide linker to be inserted at the ΔS1/S2 and ΔS2' cleavage sites of the spike protein. Mice were immunized with Phosphate buffered saline as a negative control. The timeline shows the bleeding and immunization regiment. Humoral immune responses were assessed using binding antibody ELISA to the Spike protein using serum isolated from blood collected at experimental endpoint**. (B)** Endpoint humoral antibody binding titers in response to the SARS-CoV-2 spike was not detected in the serum by ELISA**. (C)** Cellular Immune response was measured using cytokine staining assays for splenocytes collected at experimental endpoint in response to pooled S peptides for IFNγ, IL-6, IL-2, TNFα, IL-4, and IL-5. Phorbol 12-myristate 13-acetate (PMA) was utilized as a positive control, Non-Treated (NT) as a negative control, and CMV as an irrelevant control. **(D)** TNFα, IL-2, and IFNγ intracellular staining for CD4+ and CD8+ T cells collected at experimental endpoint also assessed cellular immune responses induced by the DNA vaccine constructs. Data representative of two independent experiments. Values are presented as mean ± standard deviation. *P* values were determined using the Mann-Whitney test. * $0.01 < p < 0.05$, ** $0.01 < p < 0.001$, *** $0.001 < p < 0.0001$. **** $p < 0.0001$

Figure 4. MIP3α-fusion DNA vaccines induced T-cell and antibody responses without neutralization antibody in K18-hACE2 mice

(A) K18-hACE2 transgenic mice (N=15) were intramuscularly immunized with 3 doses of 100 µg at 2-week intervals using a mouse modified Pharmajet Tropis Needle free Injector with either the pMIP3α-SARS-CoV-2-ΔC, pSARS-CoV-2-ΔC, or pMIP3α-A20-scFv DNA Vaccines. Mice were immunized with PBS as a negative control. One day prior to each immunization, mice were retro-orbitally (RO) bled. The timeline shows the bleeding and immunization regimen. Humoral immune responses were assessed using binding antibody ELISA to the Spike protein using serum isolated from blood collected at experimental endpoint. **(B)** Endpoint humoral responses measured by ELISA in each group. Mice that elicited highest Spike binding or neutralizing antibodies were color coded and matched to their corresponding number in the experimental group. **(C)** and SARS-COV-2 pseudo-virus neutralization assays. Each data point

represents serum from an individual animal (M1-M5). The assay limit of detection was defined as the lowest serum dilution tested (1:16). **(D)** Cellular immune response was measured using cytokine staining assays for splenocytes collected at experimental endpoint in response to pooled S peptides for IFNγ, IL-6, IL-2, TNFα, IL-4, and IL-5. Phorbol 12-myristate 13-acetate (PMA) was utilized as a positive control, Non Treated (NT) as a negative control, and CMV as an irrelevant control. **(E)** IFNγ intracellular staining for CD4+ and CD8+ T cells collected at experimental endpoint assessing cellular immune responses induced by the DNA vaccines. Data representative of two independent experiments. Values are presented as mean ± standard deviation. *P* values were determined using the Mann-Whitney test. * $0.01 < p < 0.05$, ** $0.01 < p < 0.001$, *** $0.001 < p < 0.0001$. **** $p < 0.0001$.

Figure 5. T Cell Immunity Alone Does Not Induce Protection against Live Virus in K18-hACE2 Mice (A) K18-hACE2 (N=64) mice were intramuscularly immunized with 3 doses of 100 µg at 2-week intervals using a mouse modified Pharmajet Tropis Needle free Injector with either the pMIP3α-SARS-CoV-2-ΔC, pSARS-CoV-2-ΔC, pMIP3α-SARS-CoV-2-linker-ΔT, or pMIP3α-A20-scFv DNA vaccines. On Day 44 of the experiment, two weeks after the third and final vaccination N=24 mice were terminally bled, and their spleen was collected for analysis. The remaining N=40 mice were then challenged with 2.8 e3 PFU of the WAS-Calu-3 SARS-CoV-2 live virus, and their survival was recorded over the course of 10 days. Humoral immune responses for N = 64 mice were assessed using binding antibody ELISA to the Spike protein **(B)** and SARS-CoV-2 live virus (WAS-Calu-3 Strain) neutralization assays **(C)** using serum isolated from blood collected at experimental endpoint. The SARS-CoV-2 neutralization assay included a virus only negative control, Rabbit Spike neutralizing antibody positive control, and a no virus control. **(D)** Cellular immune response to the vaccine was assessed via Intracellular staining cytokine analysis for N = 24 mouse CD4+ and CD8+ T cells collected at Day 44 in response to pooled S peptides for IFNγ, TNFα, and IL-2. **(E)** IFNγ ELISPOT assay also measured the cellular immune response induced by the vaccine in response to stimulation from CMV peptide pool irrelevant control, S protein peptide pools, or Concanavalin A (ConA) a positive control. Survival data was graphed over the course of 10 days post challenge in % Body Weight Loss **(F)** and % Survival **(G)** after viral challenge with 2.8 x 10^3 PFU dose of WAS-Calu-3 strain of the live SARS-CoV-2 virus. Data representative of two independent experiments. Values are presented as mean ± standard deviation. *P* values were determined using the Mann-Whitney test. * $0.01 < p < 0.05$, ** $0.01 < p < 0.001$, *** $0.001 < p < 0.0001$.

Competing Interest
The authors declare no competing interests.

Funding: Not applicable.

Contributions

S.C. and L.W.K. designed the project, oversaw the experiments, and wrote the manuscript. S.C., S.J.S., and L.W.K. contributed to the design of the vaccine construct. S.J.S. and A.A. cloned the vaccine and conducted an analysis of the sequencing data. A.A., E.O., and S.C. optimized the mouse injection protocol and carried out the immunization of the mice. Z.D. developed and optimized assays for the production of SARS-CoV-2 pseudovirus and its neutralization. M.P. and K.A. prepared and organized all mouse samples and conducted the analysis of the antibody response to the S protein. S.S., Z.D., and A.A. performed FACS and subsequently analyzed the data. Z.D., J.B., S.J.S., and A.A. conducted the data analysis and contributed to the manuscript revision.

References

1 Sievers, B. L., Cheng, M. T. K., Csiba, K., Meng, B. & Gupta, R. K. SARS-CoV-2 and innate immunity: the good, the bad, and the "goldilocks". *Cell Mol Immunol* **21**, 171-183, doi:10.1038/s41423-023-01104-y (2024).

2 Hilligan, K. L. *et al.* Bacterial-induced or passively administered interferon gamma conditions the lung for early control of SARS-CoV-2. *Nat Commun* **14**, 8229, doi:10.1038/s41467-023-43447-0 (2023).

3 Khoury, D. S. *et al.* Neutralizing antibody levels are highly predictive of immune protection from symptomatic SARS-CoV-2 infection. *Nat Med* **27**, 1205-1211, doi:10.1038/s41591-021-01377-8 (2021).

4 McMahan, K. *et al.* Correlates of protection against SARS-CoV-2 in rhesus macaques. *Nature* **590**, 630-634, doi:10.1038/s41586-020-03041-6 (2021).

5 Tarke, A. *et al.* Comprehensive analysis of T cell immunodominance and immunoprevalence of SARS-CoV-2 epitopes in COVID-19 cases. *Cell Rep Med* **2**, 100204, doi:10.1016/j.xcrm.2021.100204 (2021).

6 Sette, A. & Crotty, S. Adaptive immunity to SARS-CoV-2 and COVID-19. *Cell* **184**, 861-880, doi:10.1016/j.cell.2021.01.007 (2021).

7 Grifoni, A. *et al.* Targets of T Cell Responses to SARS-CoV-2 Coronavirus in Humans with COVID-19 Disease and Unexposed Individuals. *Cell* **181**, 1489-1501 e1415, doi:10.1016/j.cell.2020.05.015 (2020).

8 Khobragade, A. *et al.* Efficacy, safety, and immunogenicity of the DNA SARS-CoV-2 vaccine (ZyCoV-D): the interim efficacy results of a phase 3, randomised, double-blind, placebo-controlled study in India. *Lancet* **399**, 1313-1321, doi:10.1016/S0140-6736(22)00151-9 (2022).

9 Biragyn, A., Tani, K., Grimm, M. C., Weeks, S. & Kwak, L. W. Genetic fusion of chemokines to a self tumor antigen induces protective, T-cell dependent antitumor immunity. *Nat Biotechnol* **17**, 253-258, doi:10.1038/6995 (1999).

10 Biragyn, A. *et al.* Toll-like receptor 4-dependent activation of dendritic cells by beta-defensin 2. *Science* **298**, 1025-1029, doi:10.1126/science.1075565 (2002).

11 Qin, H. *et al.* Vaccine site inflammation potentiates idiotype DNA vaccine-induced therapeutic T cell-, and not B cell-, dependent antilymphoma immunity. *Blood* **114**, 4142-4149, doi:10.1182/blood-2009-05-219683 (2009).

12 Biragyn, A. *et al.* Mediators of innate immunity that target immature, but not mature, dendritic cells induce antitumor immunity when genetically fused with nonimmunogenic tumor antigens. *J Immunol* **167**, 6644-6653 (2001).

13 Thomas, S. K. *et al.* Phase I study of an active immunotherapy for asymptomatic phase Lymphoplasmacytic lymphoma with DNA vaccines encoding antigen-chemokine fusion: study protocol. *BMC Cancer* **18**, 187, doi:10.1186/s12885-018-4094-2 (2018).

14 Schiavo, R. *et al.* Chemokine receptor targeting efficiently directs antigens to MHC class I pathways and elicits antigen-specific CD8+ T-cell responses. *Blood* **107**, 4597-4605, doi:10.1182/blood-2005-08-3207 (2006).

15 Wu, F. *et al.* A new coronavirus associated with human respiratory disease in China. *Nature* **579**, 265-269, doi:10.1038/s41586-020-2008-3 (2020).

16 Crawford, K. H. D. *et al.* Protocol and Reagents for Pseudotyping Lentiviral Particles with SARS-CoV-2 Spike Protein for Neutralization Assays. *Viruses* **12**, doi:10.3390/v12050513 (2020).

17 Chiuppesi, F. *et al.* Development of a multi-antigenic SARS-CoV-2 vaccine candidate using a synthetic poxvirus platform. *Nat Commun* **11**, 6121, doi:10.1038/s41467-020-19819-1 (2020).

18 Wu, A. *et al.* Genome Composition and Divergence of the Novel Coronavirus (2019-nCoV) Originating in China. *Cell Host Microbe* **27**, 325-328, doi:10.1016/j.chom.2020.02.001 (2020).

19 Cromer, D. *et al.* Neutralising antibody titres as predictors of protection against SARS-CoV-2 variants and the impact of boosting: a meta-analysis. *Lancet Microbe* **3**, e52-e61, doi:10.1016/S2666-5247(21)00267-6 (2022).

20 Vidal, S. J. *et al.* Correlates of Neutralization against SARS-CoV-2 Variants of Concern by Early Pandemic Sera. *J Virol* **95**, e0040421, doi:10.1128/JVI.00404-21 (2021).

21 Israelow, B. *et al.* Adaptive immune determinants of viral clearance and protection in mouse models of SARS-CoV-2. *Sci Immunol* **6**, eabl4509, doi:10.1126/sciimmunol.abl4509 (2021).

22 Levin, M. J. *et al.* Intramuscular AZD7442 (Tixagevimab-Cilgavimab) for Prevention of Covid-19. *N Engl J Med* **386**, 2188-2200, doi:10.1056/NEJMoa2116620 (2022).

23 Senefeld, J. W. *et al.* Use of convalescent plasma in COVID-19 patients with immunosuppression. *Transfusion* **61**, 2503-2511, doi:10.1111/trf.16525 (2021).

24 Keeton, R. *et al.* T cell responses to SARS-CoV-2 spike cross-recognize Omicron. *Nature* **603**, 488-492, doi:10.1038/s41586-022-04460-3 (2022).

25 Madelon, N. *et al.* Robust T-Cell Responses in Anti-CD20-Treated Patients Following COVID-19 Vaccination: A Prospective Cohort Study. *Clin Infect Dis* **75**, e1037-e1045, doi:10.1093/cid/ciab954 (2022).

26 Perry, C. *et al.* Efficacy of the BNT162b2 mRNA COVID-19 vaccine in patients with B-cell non-Hodgkin lymphoma. *Blood Adv* **5**, 3053-3061, doi:10.1182/bloodadvances.2021005094 (2021).

27 Herishanu, Y. *et al.* Efficacy of the BNT162b2 mRNA COVID-19 vaccine in patients with chronic lymphocytic leukemia. *Blood* **137**, 3165-3173, doi:10.1182/blood.2021011568 (2021).

28 Yu, J. *et al.* DNA vaccine protection against SARS-CoV-2 in rhesus macaques. *Science* **369**, 806-811, doi:10.1126/science.abc6284 (2020).

29 Chai, K. M. *et al.* DNA vaccination induced protective immunity against SARS CoV-2 infection in hamsterss. *PLoS Negl Trop Dis* **15**, e0009374, doi:10.1371/journal.pntd.0009374 (2021).

30 Andrade, V. M. *et al.* INO-4800 DNA vaccine induces neutralizing antibodies and T cell activity against global SARS-CoV-2 variants. *NPJ Vaccines* **6**, 121, doi:10.1038/s41541-021-00384-7 (2021).

31 Gordy, J. T. *et al.* A SARS-CoV-2 RBD vaccine fused to the chemokine MIP-3alpha elicits sustained murine antibody responses over 12 months and enhanced lung T-cell responses. *Front Immunol* **15**, 1292059, doi:10.3389/fimmu.2024.1292059 (2024).

32 Wrapp, D. *et al.* Cryo-EM structure of the 2019-nCoV spike in the prefusion conformation. *Science* **367**, 1260-1263, doi:10.1126/science.abb2507 (2020).

33 Hsieh, C. L. *et al.* Structure-based Design of Prefusion-stabilized SARS-CoV-2 Spikes. *bioRxiv*, doi:10.1101/2020.05.30.125484 (2020).

34 Tian, J. H. *et al.* SARS-CoV-2 spike glycoprotein vaccine candidate NVX-CoV2373 immunogenicity in baboons and protection in mice. *Nat Commun* **12**, 372, doi:10.1038/s41467-020-20653-8 (2021).

35 Walls, A. C. *et al.* Elicitation of broadly protective sarbecovirus immunity by receptor-binding domain nanoparticle vaccines. *Cell* **184**, 5432-5447 e5416, doi:10.1016/j.cell.2021.09.015 (2021).

36 Shi, J. *et al.* A T cell-based SARS-CoV-2 spike protein vaccine provides protection without antibodies. *JCI Insight* **9**, doi:10.1172/jci.insight.155789 (2024).

37 Pardi, N., Hogan, M. J., Porter, F. W. & Weissman, D. mRNA vaccines - a new era in vaccinology. *Nat Rev Drug Discov* **17**, 261-279, doi:10.1038/nrd.2017.243 (2018).
38 Kocher, K. *et al.* Vaccination-induced T cell responses maintain polyclonality with high antigen receptor avidity. *Sci Immunol* **10**, eadu6730, doi:10.1126/sciimmunol.adu6730 (2025).
39 Karpus, W. J. *et al.* Differential CC chemokine-induced enhancement of T helper cell cytokine production. *J Immunol* **158**, 4129-4136 (1997).
40 Gu, L. *et al.* Control of TH2 polarization by the chemokine monocyte chemoattractant protein-1. *Nature* **404**, 407-411, doi:10.1038/35006097 (2000).

Figure 2

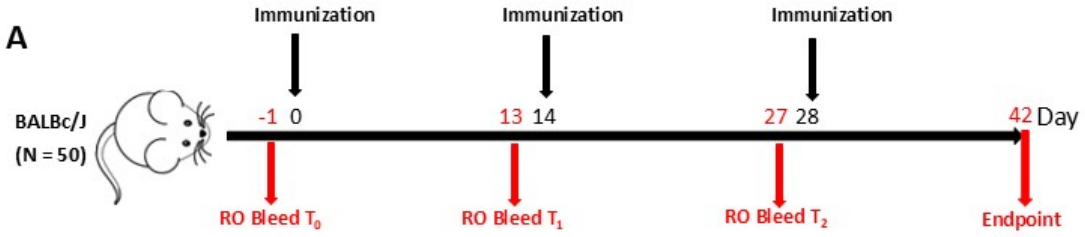

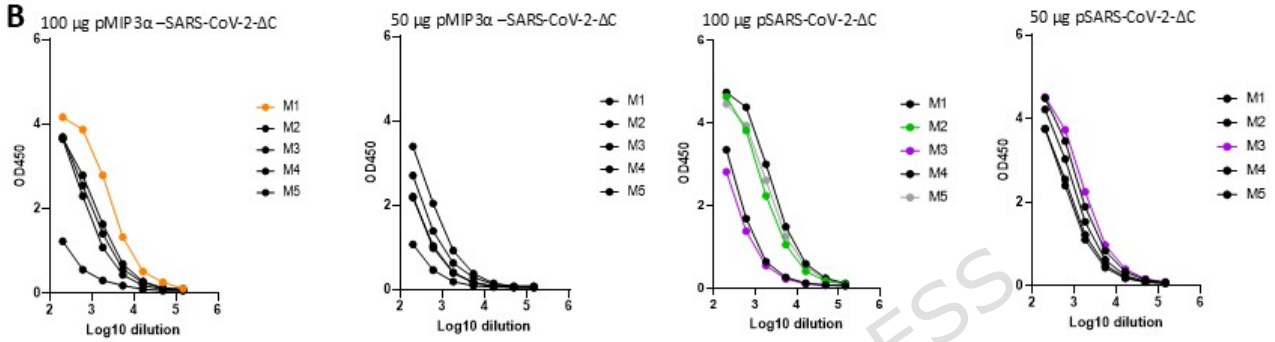

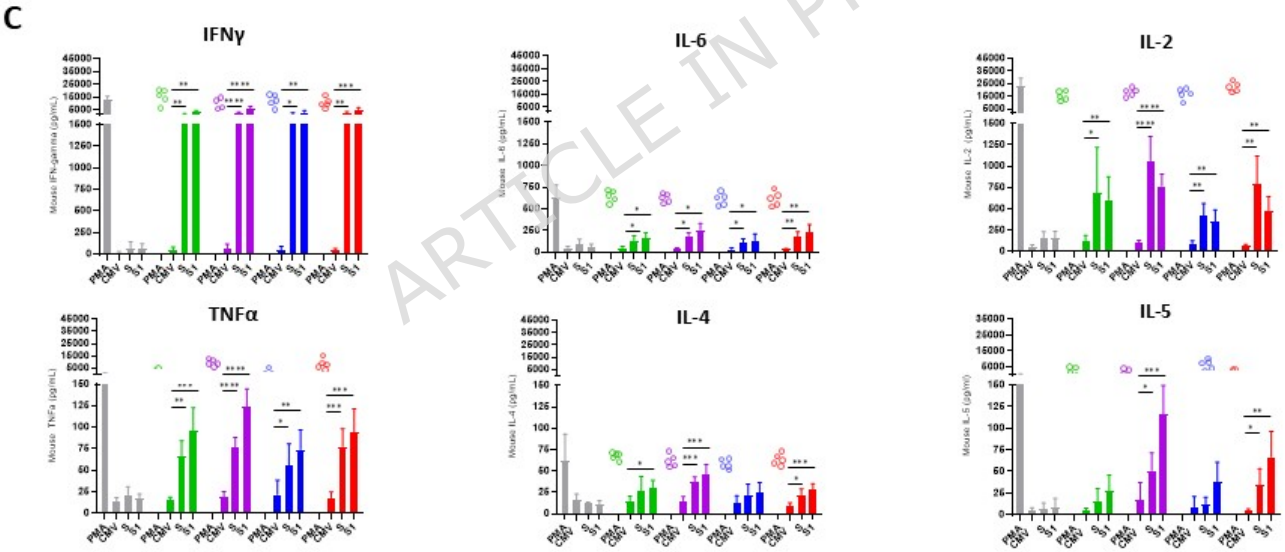

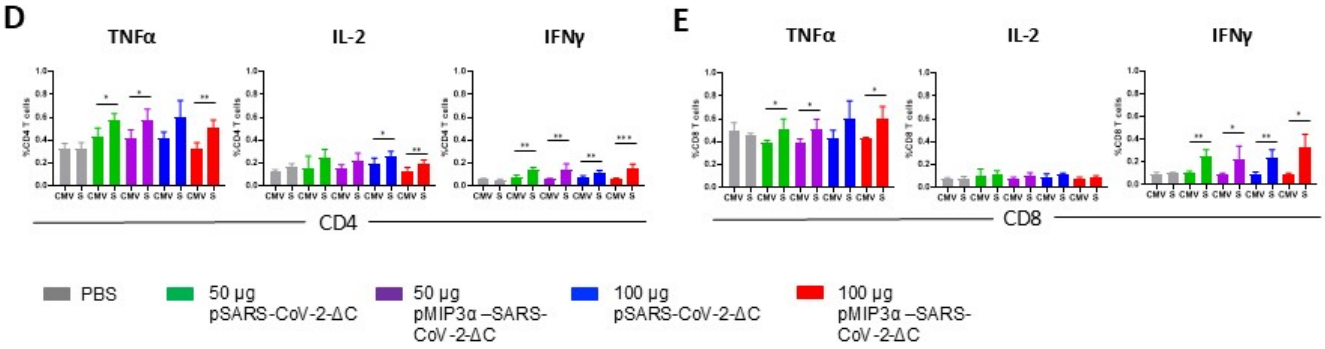

Figure 1.

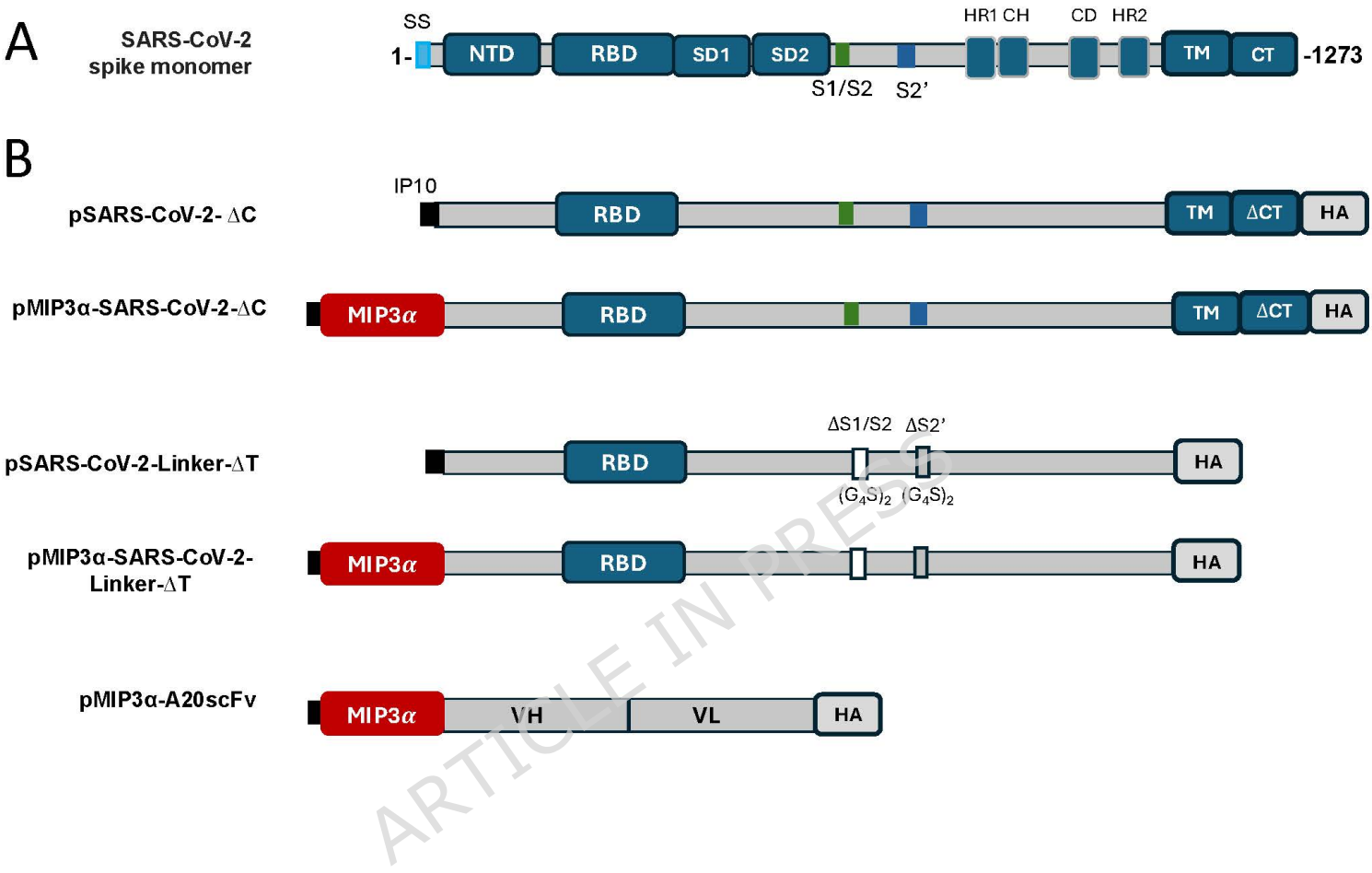

Figure 4

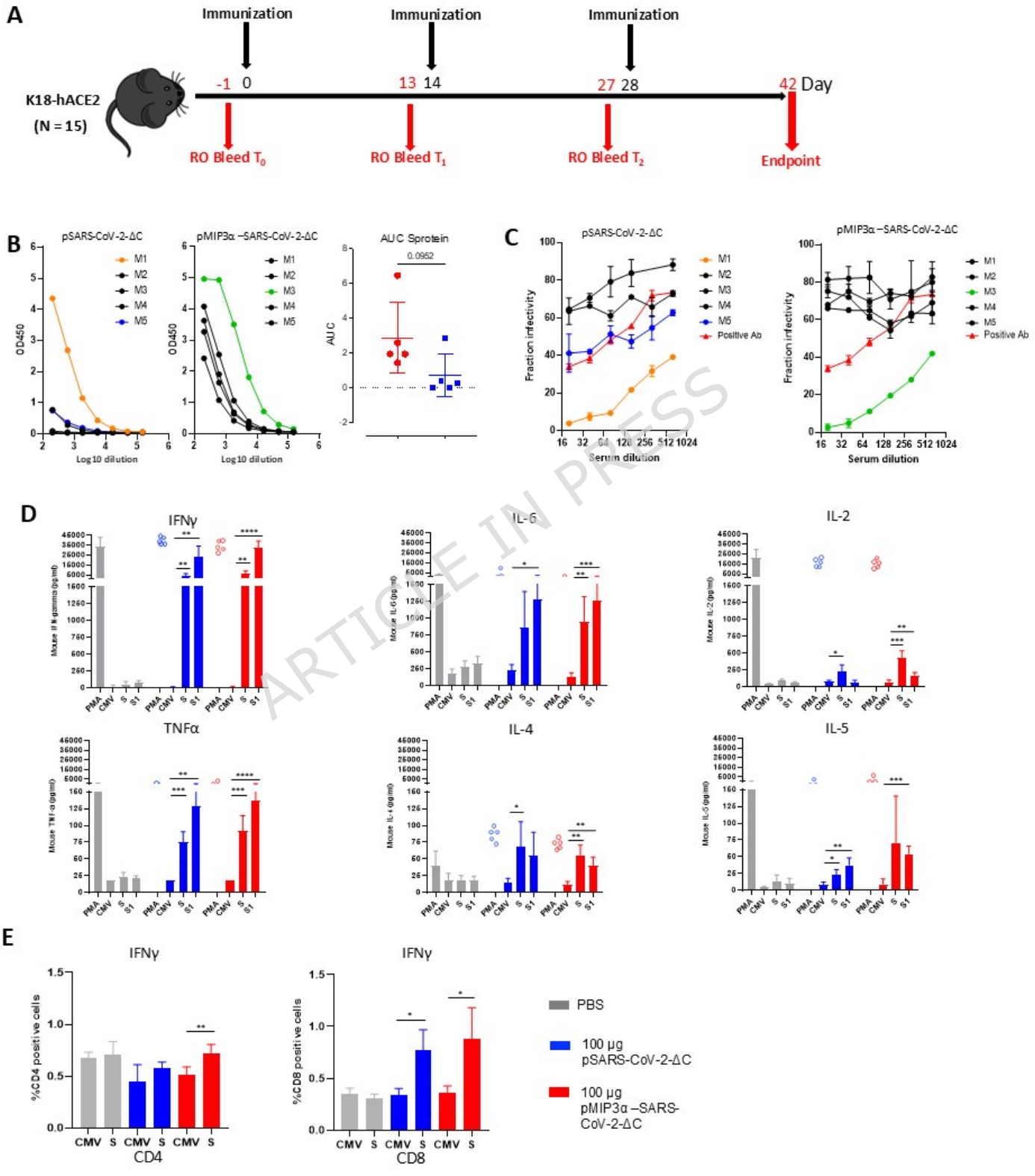

Figure 3.

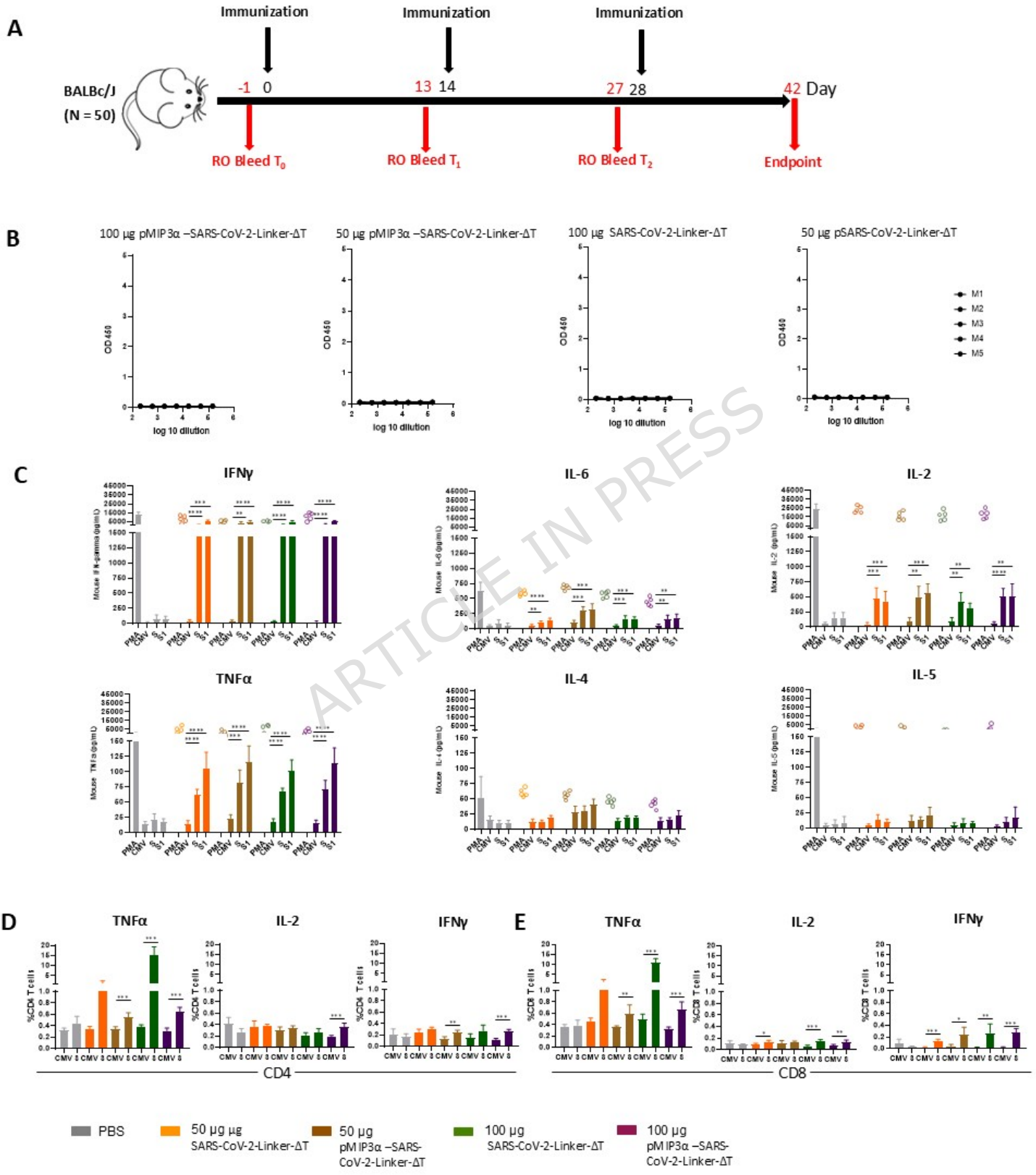

Figure 5